Placement Optimization for Multi-IRS-Aided Wireless Communications: An Adaptive Differential Evolution Algorithm

Pei-Qiu Huang, Yu Zhou, Kezhi Wang, *Senior Member, IEEE*, and Bing-Chuan Wang, *Member, IEEE*

***Abstract*—Using intelligent reflecting surfaces (IRSs) is a promising approach to enhance the performance of wireless communication systems. In this paper, the placement optimization of multi-IRSs is investigated in multi-IRS-aided wireless communication systems, with the aim of minimizing the number of IRSs subject to the average achievable data rate. Then, an adaptive differential evolution algorithm is developed to jointly optimize the number, locations, and phase shift coefficients of IRSs, in which a novel strategy is devised to adaptively select the mutation operator for each individual. Compared with other algorithms, the proposed algorithm performs well in reducing the number of IRSs while satisfying the average achievable data rate.**

***Index Terms*—Intelligent reflecting surface, placement optimization, differential evolution, mutation operator.**

I. Introduction

Using an intelligent reflecting surface (IRS) is a promising method to improve the spectral efficiency in wireless communication systems by reconfiguring the propagation environment with the aid of a large number of passive reflecting elements [1]. By adjusting the phase shifts of the reflecting elements, the reflected signals can be reconfigured to propagate towards their desired directions [2]. Thus, many researchers have attempted to develop various IRS-aided communication systems, such as mmWave communication, secure communication, and mobile edge computing. These studies mainly focus on beamforming design under the assumption that IRSs are deployed in a fixed location. In fact, IRSs can be easily installed or removed for placement/replacement as they are usually lightweight [3]. However, they do not consider placement optimization for IRS-aided wireless communications.

In order to explore the advantages of IRS-aided wireless communication systems, researchers have begun to focus on placement optimization. Mu *et al.* [4] studied the optimal placement of a single IRS for three multiple access schemes: non-orthogonal multiple access (NOMA), frequency division multiple access (FDMA), and time division multiple access (TDMA). Tang *et al.* [5] developed an aerial IRS-aided communication system, where a UAV or a balloon carries the single IRS to the intended location to mitigate jamming attacks and enhance legitimate transmissions. Zhang *et al.* [6] studied distributed and centralized placements in an IRS-assisted multi-user communication system. Specifically, the distributed placement employs available elements to form multiple distributed IRSs. Each deploys near one user and the centralized placement constructs all reflection elements into a large IRS located near the access point (AP). However, these studies do not optimize the number of IRSs. Similar to other placement problems, multi-IRS placement problems are usually NP-hard [7]. As the number of IRSs increases, it is difficult to obtain the optimal placement in a reasonable time. In addition, when the number of IRSs is not fixed, multi-IRS placement problems become more challenging.

Against this background, this paper studies the placement optimization for a multi-IRS-aided communication system with an unfixed number of IRSs. Then, a population-based heuristic algorithm, that is, differential evolution (DE) algorithm, is proposed to jointly optimize the number, locations, and phase shift coefficients of IRSs, with the aim of minimizing the number of IRSs subject to the average achievable data rate (AADR). In addition, since the performance of the DE algorithm is sensitive to the mutation operator, a novel strategy is designed to adaptively select the mutation operator for each individual. By comparison with baselines, the effectiveness of the proposed algorithm is verified in a multi-IRS-aided wireless communication system.

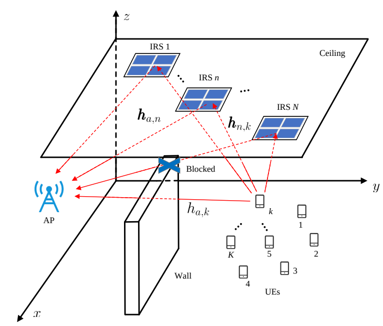

Fig. 1. A multi-IRS-aided communication system involving K UEs, n IRSs, and an AP.

II. System Model

As shown in Fig. 1, we consider a multi-IRS-aided wireless communication system in indoor environments such as

This work was supported by the National Natural Science Foundation of China under Grants 62106287. *(Corresponding authors: Kezhi Wang and Bing-Chuan Wang)*

P.-Q. Huang, Y. Zhou, and B.-C. Wang are with the School of Automation, Central South University, Changsha 410083, China (Email: pehuang@cityu.edu.hk, zyzhouyu@csu.edu.cn, bingcwang@csu.edu.cn)

K. Wang is with the Department of Computer and Information Sciences, Northumbria University, Newcastle NE1 8ST, UK. (kezhi.wang@northumbria.ac.uk)

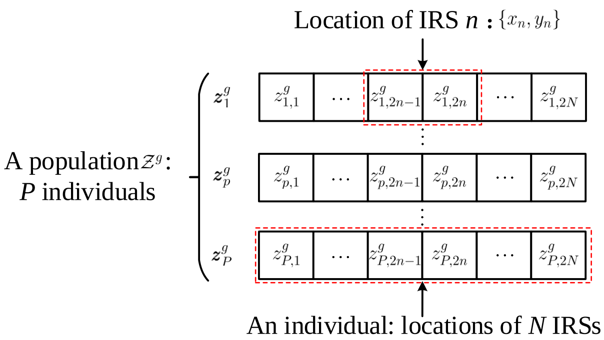

Fig. 2. A population consisting of P individuals, where each individual represents the locations of N IRSs.

stadiums and halls, where a set $\mathcal{K}$ of K single-antenna user equipments (UEs) communicate with a single-antenna AP in orthogonal time slots with the aid of a set $\mathcal{N}$ of N equal-size IRSs. We assume that each IRS placed on the ceiling is a uniform planar array equipped with M reflecting elements.

In this paper, the phase shift coefficient of IRS n is represented by $\boldsymbol{\theta}_n = [\theta_{n,1}, \theta_{n,2}, \ldots, \theta_{n,M}]^{\mathrm{T}}$; thus, the phase shift coefficient matrix of IRS n is denoted as $\boldsymbol{\Theta}_n = \mathrm{diag}\{e^{j\theta_{n,1}}, e^{j\theta_{n,2}}, \ldots, e^{j\theta_{n,M}}\}$, where j represents the imaginary unit. In addition, we denote $\boldsymbol{h}_{a,n} \in \mathbb{C}^{M\times 1}$ as the channel vector from IRS n to the AP, $\boldsymbol{h}_{n,k} \in \mathbb{C}^{M\times 1}$ as the channel vector from UE k to IRS n, and $h_{a,k} \in \mathbb{C}^{1\times 1}$ as the channel from UE k to the AP. The Rician fading channel model is used for both UE-IRS and IRS-AP links. Therefore, $\boldsymbol{h}_{a,n} \in \mathbb{C}^{M\times 1}$ is expressed as

$$\boldsymbol{h}_{a,n} = PL_{a,n}\left(\sqrt{\frac{\varepsilon}{\varepsilon+1}}\boldsymbol{a}_n(\phi_n, \theta_n) + \sqrt{\frac{1}{\varepsilon+1}}\overline{\boldsymbol{h}_{a,n}}\right), \quad (1)$$

where $PL_{a,n}$ denotes the path-loss between IRS n and the AP, ε denotes the Rician factor; $\boldsymbol{a}_n(\phi_n, \theta_n) \in \mathbb{C}^{M\times 1}$ is the array response of IRS n; ϕ_n (θ_n) denotes the azimuth (elevation) angle of departure for the link between IRS n and the AP; and $\overline{\boldsymbol{h}_{a,n}}$ denotes the non-line-of-sight components and their elements are chosen from $\mathcal{CN}(0,1)$. Similarly, $\boldsymbol{h}_{n,k}$ is expressed as

$$\boldsymbol{h}_{n,k} = PL_{n,k}\left(\sqrt{\frac{\varepsilon}{\varepsilon+1}}\boldsymbol{a}_n(\phi_n^{'}, \theta_n^{'}) + \sqrt{\frac{1}{\varepsilon+1}}\overline{\boldsymbol{h}_{n,k}}\right), \quad (2)$$

where $PL_{n,k}$ denotes the path-loss between IRS n and UE k, and $\phi_n^{'}$ ($\theta_n^{'}$) denotes the azimuth (elevation) angle of arrival for the link between IRS n and UE k. In addition, we use the Rayleigh fading model for the UE-AP link. Therefore, $h_{a,k} \in \mathbb{C}^{1\times 1}$ is expressed as

$$h_{a,k} = PL_{a,k}\overline{h_{a,k}}, \quad (3)$$

where $PL_{a,k}$ denotes the path-loss between UE k and the AP.

Then, the ergodic achievable data rate of UE k is given by

$$R_k = \mathbb{E}\left\{\log_2\left(1 + \frac{p_k\left|b_{a,k}h_{a,k} + \sum_{n=1}^{N} b_{a,n}\boldsymbol{h}_{a,n}^{\mathrm{H}}\boldsymbol{\Theta}_n\boldsymbol{h}_{n,k}\right|^2}{\sigma^2}\right)\right\}, \quad (4)$$

where p_k denotes the transmit power of UE k; σ^2 represents the noise power; $b_{a,n} = 0$ if the UE k-IRS n-AP link is blocked due to the layout of the wall, otherwise $b_{a,n} = 1$; and $b_{a,k} = 0$ if the UE k-AP link is blocked, otherwise $b_{a,k} = 1$.

For cost minimization, we jointly optimize the number, locations, and phase shift coefficients of IRSs to minimize the number of IRSs subject to the AADR for all UEs, which can be formulated as

$$\min_{N, \{x_n, y_n\}, \boldsymbol{\theta}_n} N \quad (5a)$$

$$\text{s.t.} \quad \frac{1}{K}\sum_{k=1}^{K} R_k \geq \phi, \quad (5b)$$

$$x_{min} \leq x_n \leq x_{max}, \forall n \in \mathcal{N}, \quad (5c)$$

$$y_{min} \leq y_n \leq y_{max}, \forall n \in \mathcal{N}, \quad (5d)$$

$$\max\{|x_n - x_l|, |y_n - y_l|\} \geq L, \forall n, l \in \mathcal{N}, \quad (5e)$$

$$N_{min} \leq N \leq N_{max}, \forall n \in \mathcal{N}, \quad (5f)$$

where $\{x_n, y_n\}$ denotes the location of IRS n [1], L denotes the size length of each IRS, (5b) ensures that the AADR for all UEs is less than ϕ, (5c) and (5d) represent the boundary constraints of locations of IRSs, (5e) guarantees that IRSs are not overlapped, and (5f) ensures that the number of IRSs is between $[N_{min}, N_{max}]$.

III. Proposed Algorithm

Due to the NP-hard characteristic, it is usually difficult to use deterministic algorithms to solve (5) as their computational cost is often unbearable. Therefore, population-based heuristic algorithms have been received wide attention. Among them, the DE algorithm performs better than other algorithms, such as genetic algorithm and particle swarm optimization (PSO) algorithm [8], in some complex problems due to its numerous merits including ease of implementation, simple structure, and powerful search capability. However, the performance of DE algorithm is sensitive to the mutation operator. Therefore, we design an adaptive DE algorithm to solve (5), which selects adaptively the mutation operator for each individual. The main process of the proposed algorithm is given as follows. We first set the number of IRSs to N_{min}, and then optimize the locations and phase shift coefficients of IRSs to maximize the AADR for all UEs. After several iterations, if (5b) can be satisfied, then the optimal number of IRSs is obtained; otherwise, we add one IRS and re-optimize the locations and phase shift coefficients of IRSs until (5b) is satisfied. Next, we introduce the proposed algorithm in detail.

Initialization: In order to minimize the number of IRSs, the initial number of IRSs N is set to N_{min}. Then, as shown in Fig. 2, we randomly generate an initial population $\mathcal{Z}^g = \{\boldsymbol{z}_1^g, \boldsymbol{z}_2^g, \ldots, \boldsymbol{z}_P^g\}$, in which each individual represents the locations of N IRSs:

$$\boldsymbol{z}_p^g = (z_{p,1}^g, z_{p,2}^g, \ldots, z_{p,2*N-1}^g, z_{p,2*N}^g), \forall p \in \mathcal{P}, \quad (6)$$

[1] The height optimization of IRSs is not considered as the height of the ceiling is fixed.

where $z^g_{p,2*n-1} = x_{min} + rand \cdot (x_{max} - x_{min})$ and $z^g_{p,2*n} = y_{min} + rand \cdot (y_{max} - y_{min})$ represent the location of IRS n (i.e., x_n and y_n) in individual p of iteration g ($g = 1$ at the initialization); $rand$ represents a random number uniformly distributed over $[0, 1]$; $\mathcal{P} = \{1, 2, \ldots, P\}$ represents a set of individuals; and P denotes the population size.

Mutation: The mutation operator is performed to perturb the individuals in $\mathcal{Z}^g$ to generate $\boldsymbol{v}^g_p$. The commonly used mutation operators are as follows:

1) DE/rand/1

$$\boldsymbol{v}^g_p = \boldsymbol{z}^g_{r_1} + F \cdot (\boldsymbol{z}^g_{r_2} - \boldsymbol{z}^g_{r_3}),\ \forall p \in \mathcal{P}, \tag{7}$$

2) DE/rand/2

$$\boldsymbol{v}^g_p = \boldsymbol{z}^g_{r_1} + F \cdot (\boldsymbol{z}^g_{r_2} - \boldsymbol{z}^g_{r_3}) + F \cdot (\boldsymbol{z}^g_{r_4} - \boldsymbol{z}^g_{r_5}),\ \forall p \in \mathcal{P}, \tag{8}$$

3) DE/current-to-rand/1

$$\boldsymbol{v}^g_p = \boldsymbol{z}^g_p + F \cdot (\boldsymbol{z}^g_{r_1} - \boldsymbol{z}^g_p) + F \cdot (\boldsymbol{z}^g_{r_2} - \boldsymbol{z}^g_{r_3}),\ \forall p \in \mathcal{P}, \tag{9}$$

where r_1, r_2, r_3, r_4, and r_5 are five distinct integers randomly selected from $[1, P]$ and are also different from p, and F is the scaling factor.

To generate each $\boldsymbol{v}^g_p$, the roulette wheel method is used to select one of the aforementioned three mutation operators based on a weight vector $\boldsymbol{w}^g = [w^g_{p,1}, w^g_{p,2}, w^g_{p,3}]$, where $\boldsymbol{w}^g$ is initially set to $[\frac{1}{3}, \frac{1}{3}, \frac{1}{3}]$, and $w^g_{p,1}$, $w^g_{p,2}$, and $w^g_{p,3}$ represent the weights of three mutation operators, respectively.

Crossover: To enhance the potential diversity of the population, a crossover operator is then performed on $\boldsymbol{v}^g_p$ and $\boldsymbol{z}^g_p$ to generate $\boldsymbol{u}^g_p$. The commonly used binomial crossover is as follows:

$$u^g_{p,n} = \begin{cases} v^g_{p,n}, & \text{if } rand_n \leq CR \text{ or } n = n_{rand}, \\ z^g_{p,n}, & \text{otherwise}, \end{cases} \tag{10}$$

where n_{rand} denotes a random integer selected from $[1, 2*N]$ to make sure that $\boldsymbol{u}^g_p$ is different from $\boldsymbol{z}^g_p$ in at least one dimension, $rand_n$ denotes a uniformly distributed random number over $[0, 1]$ for each n, and CR denotes the crossover control parameter.

Beamforming design: In order to evaluate the fitness value of $\boldsymbol{u}^g_p$, we need to optimize the phase shift coefficients of IRSs corresponding to $\boldsymbol{u}^g_p$. Similar to [9], we adopt the quantitative passive beamforming approach for optimizing the phase shift coefficients of IRSs. Indeed, (1) and (2) can be respectively transformed into the following forms:

$$\boldsymbol{h}_{a,n} = \left[|\boldsymbol{h}_{a,n}|e^{jw_{a,n,1}}, |\boldsymbol{h}_{a,n}|e^{jw_{a,n,2}}, \ldots, |\boldsymbol{h}_{a,n}|e^{jw_{a,n,M}}\right]^{\mathrm{T}}, \tag{11}$$

and

$$\boldsymbol{h}_{n,k} = \left[|\boldsymbol{h}_{n,k}|e^{jw_{n,k,1}}, |\boldsymbol{h}_{n,k}|e^{jw_{n,k,2}}, \ldots, |\boldsymbol{h}_{n,k}|e^{jw_{n,k,M}}\right]^{\mathrm{T}}, \tag{12}$$

where $|\boldsymbol{h}_{a,n}|$ and $|\boldsymbol{h}_{n,k}|$ represent the magnitude of $\boldsymbol{h}_{a,n}$ and $\boldsymbol{h}_{n,k}$, respectively; $e^{jw_{a,n,m}}$ and $e^{jw_{n,k,m}}$ represent the phase shifts of $h_{a,n,m}$ and $h_{n,k,m}$, respectively.

It can be seen that maximizing the achievable data rate can be achieved by coherently combining signals from different paths at the AP because these coherent signal constructions can maximize the received signal power. Therefore, when UE

Algorithm 1: Proposed algorithm

input : N_{min}, g_{max}, and P
output: N_{best}, $\boldsymbol{z}_{best}$, and $\boldsymbol{\theta}_{best}$

Initialize $N = N_{min}$;
repeat
  Initialize $g = 1$, $\mathcal{Z}^g = \{\boldsymbol{z}^g_1, \boldsymbol{z}^g_2, \ldots, \boldsymbol{z}^g_P\}$, and $\boldsymbol{w}^g = [\frac{1}{3}, \frac{1}{3}, \frac{1}{3}]$;
  Optimize the phase shift coefficients of IRSs for each $\boldsymbol{z}^g_p$;
  Calculate the fitness value of each $\boldsymbol{z}^g_p$;
  for $g = 2 : g_{max}$ **do**
    for $p = 1 : P$ **do**
      Select a mutation operator based on $\boldsymbol{w}^g$;
      Perform the mutation operator to perturb the indivduals in $\mathcal{Z}^g$ to generate $\boldsymbol{v}^g_p$; `// Mutation`
      Perform the crossover operator on $\boldsymbol{v}^g_p$ and $\boldsymbol{z}^g_p$ to generate $\boldsymbol{u}^g_p$; `// Crossover`
      Optimize the phase shift coefficients of IRSs for $\boldsymbol{u}^g_p$; `// Beamforming design`
      Calculate the fitness value of $\boldsymbol{u}^g_p$; `// Fitness evaluation`
      Perform the selection operator to obtain $\boldsymbol{z}^{g+1}_p$; `// Selection`
      Update $\boldsymbol{w}^g$; `// Weight update`
    end
  end
  Record $N_{best} \leftarrow N$, $\boldsymbol{z}_{best} \leftarrow$ the best individual in $\boldsymbol{z}^{g+1}_p$, and $\boldsymbol{\theta}_{best} \leftarrow$ the optimal phase shift coefficients of IRSs corresponding to $\boldsymbol{z}_{best}$;
  Update $N \leftarrow N + 1$; `// Number update`
until $f(\boldsymbol{z}_{best}) \leq 0$;

k communicates with the AP, the optimal phase shift of shift element m of IRS n can be obtained by

$$\theta^*_{n,m} = w_{n,k,m} + w_{a,n,m}. \tag{13}$$

Fitness evaluation: Then, the Monte Carlo method is used to evaluate the fitness value of $\boldsymbol{u}^g_p$ via the following fitness function:

$$f(\boldsymbol{u}^g_p) = -\frac{1}{K}\sum_{k=1}^{K} R_k(\boldsymbol{u}^g_p) + \phi. \tag{14}$$

(14) is used to measure the AADR for all UEs. The smaller the $f(\boldsymbol{u}^g_p)$ is, the larger the AADR for all UEs is. If $f(\boldsymbol{u}^g_p) \leq 0$, then (5b) is satisfied. Note that if $\boldsymbol{u}^g_p$ cannot satisfy (5e), then $f(\boldsymbol{u}^g_p)$ is penalized and set to a very large number (e.g., 10^6).

Selection: Finally, the selection operator is performed to select the better one of $\boldsymbol{u}^g_p$ and $\boldsymbol{z}^g_p$ to the next iteration based on their fitness values:

$$\boldsymbol{z}^{g+1}_p = \begin{cases} \boldsymbol{u}^g_p, & \text{if } f(\boldsymbol{u}^g_p) \leq f(\boldsymbol{z}^g_p), \\ \boldsymbol{z}^g_p, & \text{otherwise}. \end{cases} \tag{15}$$

Weight update: After performing the selection operator, we need to update $\boldsymbol{w}^g$. To this end, we update the score π_p^g of the mutation operator in the following three cases:

$$\pi_p^g = \begin{cases} \gamma_1, & \text{if } f(\boldsymbol{z}_p^{g+1}) < f(\boldsymbol{z}_{best}), \\ \gamma_2, & \text{if } f(\boldsymbol{z}_p^{g+1}) \geq f(\boldsymbol{z}_{best}) \ \& \ f(\boldsymbol{z}_p^{g+1}) < f(\boldsymbol{z}_p^g), \\ \gamma_3, & \text{if } f(\boldsymbol{z}_p^{g+1}) \geq f(\boldsymbol{z}_p^g), \end{cases} \tag{16}$$

where γ_1, γ_2, and γ_3 are three preset parameters used to represent different increased scores, $\gamma_1 > \gamma_2 > \gamma_3 \geq 0$, and $\boldsymbol{z}_{best}$ represents the best individual so far. The first case means that $\boldsymbol{z}_p^{g+1}$ has excellent performance. Therefore, in this paper, we add the selection probability of the mutation operator by setting γ_1 to a large value. The second case means that the mutation operator slightly improves the performance of $\boldsymbol{z}_p^g$. Therefore, we set γ_2 to a small positive number. In addition, the third case means that the mutation operator cannot improves the performance of $\boldsymbol{z}_p^g$. Therefore, we set γ_3 to zero.

Then, we update the weight of the selected mutation operator as follows:

$$w_{p,i}^{g+1} = (1-\lambda)w_{p,i}^g + \lambda\pi_p^g, \forall p \in \mathcal{P}, i \in \{1,2,3\}, \tag{17}$$

where $\lambda \in [0,1]$ is a reaction factor.

Number update: After g_{max} iterations, if the best individual in the population still cannot satisfy (5b) (i.e., $f(\boldsymbol{z}_{best}) > 0$), then we add one IRS and re-optimize the locations and phase shift coefficients of IRSs. This process is repeated until (5b) is satisfied. Finally, the optimal number, locations, and phase shift coefficients of the IRSs can be obtained.

Algorithm 1 summarizes the proposed algorithm for placement optimization in multi-IRS-aided wireless communications. The computational complexity of the proposed algorithm is given by $\mathcal{O}\left(2(N_{max} - N_{min} + 1) \cdot g_{max} \cdot P \cdot N_{max}\right)$.

IV. Extension To Time Allocation

When extending our work to the case with time allocation to different users, we need to study the joint optimization of placement and time allocation. This problem can be decomposed into two sub-problems and solved through an iterative mechanism. Specifically, the locations and phase shift coefficients of IRSs are obtained by using the proposed DE algorithm. Then, given fixed locations and phase shift coefficients of IRSs, the time allocation problem can be formulated as

$$\min_{t_k} -\frac{1}{K}\sum_{k=1}^{K} t_k R_k + \phi \tag{18a}$$

$$\text{s.t.} \quad t_k R_k \geq \phi_{k,min}, \forall k, \tag{18b}$$

$$\sum_{k=1}^{K} t_k \leq T. \tag{18c}$$

where the minimal data rate for UEs is given in (18b) and (18c) ensures that the total allocated time does not exceed the available time T for transmission.

It is clear that (18) is a linear programming problem, which can be easily solved. Note that, (18) has no solution if $\sum_{i=1}^{K} \frac{\phi_{i,min}}{R_i} > T$. If $\sum_{i=1}^{K} \frac{\phi_{i,min}}{R_i} \leq T$, after sorting UEs as $R_1 \geq R_2 \geq \cdots \geq R_k$, we can obtain a closed-form solution of Problem (18) as follows:

$$t_k^* = \begin{cases} T - \sum_{i=2}^{K} \frac{\phi_{i,min}}{R_i}, & \text{if } k = 1, \\ \frac{\phi_{i,min}}{R_i}, & \text{if } k \neq 1. \end{cases} \tag{19}$$

TABLE I
Parameter Settings.

Symbol	Value	Symbol	Value	Symbol	Value	Symbol	Value
K	20	L	0.3 m	M	100	p_k	1 mW
ε	10	σ^2	-80 dBm	N_{min}	1	N_{max}	10
P	10	g_{max}	100	F	0.9	CR	0.9
λ	0.9	γ_1	13	γ_2	3	γ_3	0

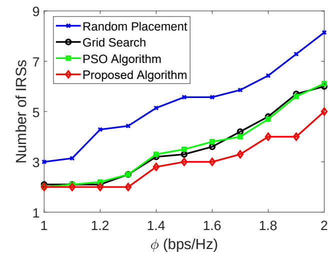

Fig. 3. Average number of IRSs obtained by the proposed algorithm and the baselines over twenty runs.

V. Experimental Studies

In this section, a multi-IRS-aided wireless communication system is used to evaluate the performance of the proposed algorithm. In the studied system, all UEs are randomly distributed in a square area with vertices [0, 0, 0], [0, 10, 0], [0, 10, 0], and [10, 10, 0] m, and the IRSs are placed in a square area with vertices [0, 0, 10], [0, 10, 10], [10, 0, 10], and [10, 10, 10] m. In addition, we set the locations of AP to [5, -10, 1] m and the location of the wall is determined by four vertices [0, 0, 0], [0, 0, 2.25], [10, 0, 2.25], [10, 0, 0] m. As for the channels, the path loss in dB is expressed as $PL = PL_0 - 10\beta \log(\frac{d}{d_0})$, where $PL_0 = 30$ dB is the path loss at the reference distance $d_0 = 1$ m; d denotes the distance from the transmitter to the receiver; and the path-loss exponents of the UE-IRS-AP link and the UE-AP link are set to $\beta = 2.2$ and $\beta = 4.0$, respectively. The remaining parameters are summarized in Table I.

Additionally, three algorithms are adopted as baselines. (1) **Random placement:** We first set the initial number of IRSs N to N_{min} and randomly place N IRSs. If (5b) is not satisfied, then we add N by one and randomly regenerate the locations of N IRSs. This process is repeated until (5b) is satisfied; (2) **Grid search:** We first divide the square area, where the IRSs are placed, into 100 grids and set the initial number of IRSs N to N_{min}. Then, the orthogonal experimental design is used to determine the locations of N IRSs. The following steps are the same as those of the random placement; and (3) **PSO algorithm:** Similar to the DE algorithm, the PSO algorithm is also a population-based heuristic algorithm, which is motivated by the collective behavior of flocks of birds

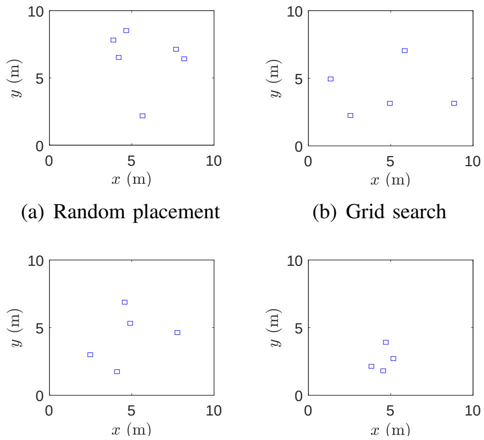

(a) Random placement (b) Grid search

(c) PSO algorithm (d) Proposed algorithm

Fig. 4. Placements obtained by the proposed algorithm and the baselines when $\phi = 1.8$ bps/Hz.

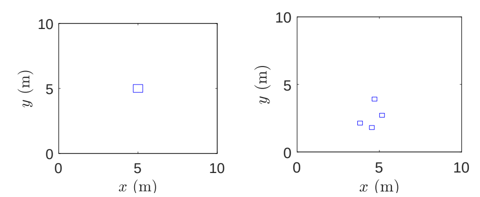

(a) Centralized placement (b) Distributed placement

Fig. 5. Centralized and distributed placements with 400 reflecting elements.

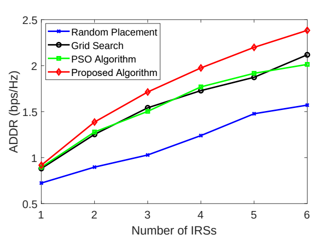

Fig. 6. Average values of the AADR obtained by the proposed algorithm and the baselines over twenty runs.

[8]. Twenty independent runs are implemented on both the proposed algorithm and the baselines.

As shown in Fig. 3, we present the average number of IRSs obtained by the proposed algorithm and the baselines over twenty runs. We see that the proposed algorithm achieves fewer IRSs, followed by PSO algorithm, while the random placement needs the most IRSs. The reason why the performance of the PSO algorithm is worse than that of the proposed algorithm is that it more easily falls into the local optimum. Since the area where the IRSs are located is restricted, the grid search does not perform well. In addition, the poor performance of the random placement is attributed to the fact that it does not consider the distribution of UEs.

In Fig. 4, we present the placement obtained by the proposed algorithm and the baselines when $\phi = 1.8$ bps/Hz. The positions of IRSs are closer in the placement obtained by the proposed algorithm compared with the baselines Furthermore, we compare the centralized and distributed placements with 400 reflecting elements. The IRS under centralized placement is located at the center of UEs (i.e., [5, 5, 0] m). In addition, the distributed placement is obtained by the proposed algorithm. The centralized and distributed placements are shown in Fig. 5, and the average values of the AADR over twenty runs are 1.83 bps/Hz and 1.98 bps/Hz, respectively. Obviously, the distributed placement performs better than the centralized placement.

Fig. 6 presents the average values of the AADR obtained by the proposed algorithm and the baselines over twenty runs. The proposed algorithm obtains the highest AADR in all cases. In addition, the grid search performs similarly to the PSO algorithm, while the random placement has the worst performance.

VI. Conclusions

This paper investigated the placement optimization for multi-IRS-aided wireless communications. Then, an adaptive DE algorithm was proposed to minimize the number of IRSs subject to the AADR by jointly optimizing the number, locations, and phase shift coefficients of IRSs. The effectiveness of the proposed algorithm was verified by comparison with other algorithms. The results showed that the proposed algorithm can reduce the number of IRSs while stratifying the AADR.

References

[1] C. Pan, H. Ren, K. Wang, J. F. Kolb, M. Elkashlan, M. Chen, M. Di Renzo, Y. Hao, J. Wang, A. L. Swindlehurst *et al.*, “Reconfigurable intelligent surfaces for 6g systems: Principles, applications, and research directions,” *IEEE Communications Magazine*, vol. 59, no. 6, pp. 14–20, 2021.

[2] Y. Omid, S. M. Shahabi, C. Pan, Y. Deng, and A. Nallanathan, “Low-complexity robust beamforming design for IRS-aided miso systems with imperfect channels,” *IEEE Communications Letters*, vol. 25, no. 5, pp. 1697–1701, 2021.

[3] Q. Wu, S. Zhang, B. Zheng, C. You, and R. Zhang, “Intelligent reflecting surface-aided wireless communications: A tutorial,” *IEEE Transactions on Communications*, vol. 69, no. 5, pp. 3313–3351, 2021.

[4] X. Mu, Y. Liu, L. Guo, J. Lin, and R. Schober, “Joint deployment and multiple access design for intelligent reflecting surface assisted networks,” *IEEE Transactions on Wireless Communications*, vol. 20, no. 10, pp. 6648–6664, 2021.

[5] X. Tang, D. Wang, R. Zhang, Z. Chu, and Z. Han, “Jamming mitigation via aerial reconfigurable intelligent surface: Passive beamforming and deployment optimization,” *IEEE Transactions on Vehicular Technology*, vol. 70, no. 6, pp. 6232–6237, 2021.

[6] S. Zhang and R. Zhang, “Intelligent reflecting surface aided multi-user communication: Capacity region and deployment strategy,” *IEEE Transactions on Communications*, vol. 69, no. 9, pp. 5790–5806, 2021.

[7] M. L. Brandeau and S. S. Chiu, “An overview of representative problems in location research,” *Management Science*, vol. 35, no. 6, pp. 645–674, 1989.

[8] J. Kennedy and R. Eberhart, “Particle swarm optimization,” in *Proceedings of ICNN’95 - International Conference on Neural Networks*, vol. 4, 1995, pp. 1942–1948.

[9] S. Li, B. Duo, X. Yuan, Y.-C. Liang, and M. Di Renzo, “Reconfigurable intelligent surface assisted uav communication: Joint trajectory design and passive beamforming,” *IEEE Wireless Communications Letters*, vol. 9, no. 5, pp. 716–720, 2020.